Project Title:

MODELING THE DISPERSION OF VAPOR AND AEROSOL PARTICULATES IN THE ATMOSPHERIC BOUNDARY LAYER

PI: Steven Chai and Darko Koracin

Consultant: Leif Enger, Matthias Mohr

1. Introduction

The turbulent flow in the atmosphere is so complex and ranges over such a large range of scales that even if we were able to describe its detailed structure it would be practically impossible to simulate it. The study of turbulent flow is therefore focused on describing the statistical characteristics of the turbulence. One makes the assumption that the turbulent flow can be separated into a slowly varying mean component and a rapidly varying turbulent component. To model the planetary boundary layer, one needs to average the processes over the grid volume and the time step. Averaging the equations of motions, humidity, heat and concentrations generates a number of second-order moments. Classical K-theory is the simplest way to deal with this "closure" problem. It is analogous to molecular diffusion and postulates the various moments, interpreted as fluxes, to be proportional to the local gradients of the corresponding mean fields. It is possible to write down formal balance equations for all the second order moments. These equations will then contain a number of new, unknown, third-order moments. Formal equations can be written for each of these, but this generates a still larger amount of unknown moments, fourth-order moments etc ad infinitum.

All meso-scale models have to include information on the large-scale synoptic weather situation, either by using measured data from the studied area or by using data from a large-scale synoptic model. The latter can be a global model, a regional model or in some cases, the mesoscale model itself. The last procedure is usually referred to as nesting of the mesoscale model in itself.

The mathematical procedure for both driving the mesoscale model with data from larger-scale models and nesting the meso-scale model in itself is essentially identical. The method used in the MIUU model is described in Section 2.

2. The dynamic models

As input to the dispersion model, the following sets of turbulent fields characterized by differing complexities of atmospheric information are used:

- Measured wind profiler data
- CALMET, diagnostic model
- MM5, first-order closure (K-theory) model
- MIUU, second-order closure model

The first set was obtained by interpolation and extrapolation of data measured by wind profilers at Mohave Power Project (MPP), Meadview, Overton Beach, and Truxton. The wind profilers were located within the range of 150-200 km around the source. The measurement data were interpolated and extrapolated for a 300 by 300 km² domain with a resolution of 3 km between grid points.

The second set was derived from the diagnostic atmospheric model CALMET (Scire *et al.*, 1995) and will be indicated as CALMET fields. CALMET produces gridded fields of wind components, mixing heights, stability categories, micrometeorological parameters, and precipitation. The model uses standard hourly surface and twice-daily upper air observations as input. It can also use specially collected meteorological data such as hourly radar wind profiler data, or a combination of various types of data. CALMET can also use outputs from different atmospheric models such as MM5 as inputs. In our case upper air data from three wind profilers located at MPP, MEAD, and TRUX were used as inputs for the CALMET simulation (Vimont, 1997). The model was run with a domain of 300 km west-east by 400 km south-north, using a spatial resolution of 5 km. Wind fields were simulated at 12 vertical levels from the surface to 3 km AGL.

The third set, referred to as MM5 wind fields, was obtained for a limited period, Julian days 219 through 226, 1992. The MM5 model was developed by the National Center for Atmospheric Research and Pennsylvania State University (Grell *et al.*, 1995). Since the late 1970s, this model has been used in many studies of regional and mesoscale weather phenomena. Mesoscale Model 5 preprocessing includes an advanced objective analysis of the synoptic data from the global network and provides detailed initial and boundary conditions for simulations. We used a non-hydrostatic version of MM5 with a 3 km horizontal resolution. The model domain consisted of 124 x 91 horizontal grid points and 35 vertical levels. The grid was centered at 35.7° N and 114.0° W. In order to include more upper-air measurements in the initialization process, an expanded grid of 60 km beyond the boundary of the model grid was used. Due to high horizontal and vertical resolution as well as a large number of grid points, the model required significant computational effort. Because of this limitation, only a selected episode from 7 through 14 August 1992 was simulated by using MM5 over a specific domain.

The fourth set, referred as the MIUU-model's wind and turbulence fields, is a non-linear, three-dimensional, hydrostatic, incompressible numerical modeling system with second-order closure that has been developed at Meteorological Institute Uppsala University (MIUU), Sweden, during the last two decades. The modeling system consists of a number of nested models. The outermost model is driven by a large-scale synoptic model – in this study the NCEP/NCAR Reanalysis Model has been used. The inner models are driven by the same pressure fields and by employing the forcing of the mean values from the larger model at the boundaries. The dynamic models consist of prognostic equations for the

horizontal wind components, liquid water potential temperature, mixing ratio of total water, and turbulence kinetic energy. Simulations have been performed for several nested models to receive wind and turbulence fields with horizontal resolutions of 6 km, 3 km and 1.5 km.

2a. The Flow Relaxation Scheme (FRS):

The introduction of large-scale synoptic data into a meso-scale model is an extremely complex and mathematically ill posed problem. Several methods have been proposed in the past, including a number of open boundary conditions, different radiation conditions and a sponge-type boundary condition named the Flow Relaxation Scheme (FRS).

Davies (1976) was the first scientist to propose the FRS technique. Davies (1983) also tested the method for atmospheric models and compared it against several other methods.

Jensen (1998) discussed and compared a number of different boundary conditions using a limited-area ocean model, and found that the FRS performed best in most cases.

The philosophy behind the FRS is to relax the interior solution in the vicinity of the boundary towards an external solution, here called U_{ext}, V_{ext}, Θ_{ext} and Q_{ext}, where U and V are the horizontal wind components, Θ is the potential temperature, and Q is the specific humidity. The FRS forces the above named quantities to the value of the external solution and works at the same time as a sponge condition. The FRS thus prevents outward propagating waves from reflecting backwards into the model interior.

The implementation of the FRS into the model equations is done by adding a Newtonian term to the prognostic equations within the outermost model grid points. The equations are modified to

$$\frac{\partial U}{\partial t} = \ldots - \alpha_i (U - U_{ext})$$

$$\frac{\partial V}{\partial t} = \ldots - \alpha_i (V - V_{ext})$$

$$\frac{\partial \Theta}{\partial t} = \ldots - \alpha_i (\Theta - \Theta_{ext})$$

$$\frac{\partial Q}{\partial t} = \ldots - \alpha_i (Q - Q_{ext})$$

where the dots denote all the other terms in the prognostic equations, α_i the flow-relaxation coefficient and U_{ext}, V_{ext}, Θ_{ext} and Q_{ext} the values of the external solution, (i.e. the values from a global atmospheric model, a regional atmospheric model, or the meso-scale model itself when nesting is applied).

The flow-relaxation coefficient α_i is zero in the interior of the model and non-zero at the lateral boundaries of the model. In the current version of the model, four grid-points are

used for the FRS. To minimize reflection of gravity waves at the lateral boundaries, it is important to choose a convenient function for the values of α_i.

In the current version of the model, the function

$$\alpha_i = \frac{1.5 \cdot 10^{-3}}{i^2}$$

for $i = 1,...,4$ is applied for the flow-relaxation coefficient. Here, the index i denotes the number of the grid-point counted from the lateral boundary.

Since the correct solution in the fine-grid limited area atmospheric model is strongly determined by regional factors, such as orographic forcing, forcing by land-use heterogeneity and so on, it can not be adopted solely from the large-scale atmospheric model. Instead, the correct solution is a combination of the large-scale atmospheric conditions together with the prevailing regional factors.

To take both factors into consideration, the flow-relaxation coefficient is also varies with height. It approaches zero at the ground, and reaches its maximum value, α_i, at 5000 m above ground. In between these two levels, the coefficient is varied linearly with height.

The philosophy behind this innovation is that the large-scale atmospheric conditions should determine the solution at higher atmospheric levels, whereas the regional factors should determine the solution close to the surface.

The FRS is applied to all the above named variables at the vertical lateral boundaries. At the top of the model, however, the FRS is only applied to the horizontal wind components. Additionally, the pressure field is varied in all model grid-points according to the large-scale atmospheric conditions.

2b. The external solution and the large-scale atmospheric conditions:

For the external solution and the large-scale atmospheric conditions, global atmospheric Reanalysis data are used. The data are freely available via FTP from "The NCEP/NCAR Reanalysis Project".

The NCEP/NCAR Reanalysis Project was an effort to reanalyze historical data using state-of-the-art global atmospheric models. The NMC Development Division (1988) provides a comprehensive documentation of the 1988 version of the model. Kanamitsu (1989), Kanamitsu et al. (1991), and Kalnay et al. (1990) summarize subsequent model development.

The "NCEP/NCAR Reanalysis Project" used a grid with 2.5 x 2.5 degree resolution in latitude/longitude for air temperature, geopotential height, specific humidity, the Omega vertical velocity, and the horizontal wind components U and V. The grid consists of 144 x 73 grid-points.

For the other variables, a spectral triangular 62 (T62) Gaussian grid consisting of 192x94 grid-points is used. This is roughly equivalent to 2 x 2 degree resolution in latitude/longitude. For radiation, a Gaussian grid with 128 x 62 grid points in longitude/latitude is used in the model.

2c. The interpolation procedure:

To use the NCEP/NCAR Reanalysis data in a meso-scale model, the data have to be interpolated to the grid of the meso-scale model. Firstly, the data were interpolated horizontally to the grid of the meso-scale model. This was done using already existing routines, applying the Spline interpolation method.

The horizontally interpolated data was then read by the model and interpolated linearly in the vertical direction to the grid of the meso-scale model. Finally, these data were linearly interpolated in time to prescribe the time variation of the large-scale atmospheric conditions.

These data were then used, together with the equations above, to compute the time tendency of the respective variable in the meso-scale model.

Using this method it was possible to run the model for 216 hours, covering the time from 12 UTC on August 5, 1992, to 12 UTC on August 14, 1992.

3. Dispersion models

Air pollution modeling research has proceeded along several principally different lines; Gaussian model approach, Diffusion equation model approach (Eulerian), and Lagrangian particle model approach. In this proposal, tests with a Eulerian dispersion model and a Gaussian dispersion model will be performed.

The Eulerian dispersion model is a higher-order closure model that is very computer demanding and time consuming. This model should therefore only be used for special investigations. In this project we will use it for a shorter simulation period during the summer intensive study. As it needs all the second order moments from a dynamic model, only a higher-order closure dynamic model (in our case the MIUU-model) can be used as a data creator to the higher-order closure dispersion model (HOCD). The HOCD solves prognostically the mean concentration of atmospheric pollutants, as well as the second-order moments, which include fluctuating concentration. Enger and Koracin (1995) demonstrated that a higher-order dispersion model is able to predict a detailed structure of SO_2 concentrations and that the results compared well with surface and aircraft measurements. Since this higher-order closure model is fairly complex and the computational time is even longer than for the fully prognostic atmospheric model, it is not practical for longer-term (week-month-year) dispersion calculations. Therefore, a semi-Gaussian, trajectory-type dispersion model (SGTD), which is more suitable for longer-term dispersion estimates, is tested as well.

The semi-Gaussian model calculates trajectories for the plume from the simulated wind fields and approximates the concentration fields with a bi-Gaussian distribution. Since the concentration field at a certain time will be built up of several trajectories, a Gaussian distribution of the concentration around a trajectory does not mean that the concentration field must look Gaussian. The wind-direction shear not only influences the relative lateral spread but also affects the position of the plume centerline. Large wind-direction shear is common in the studied area, which means that the plume can split and proceed in different directions. One simple way to take this effect into consideration is to calculate trajectories at different heights within the plume. In this study we have calculated trajectories at two heights, one for the center of mass of the plume and one for some distance below that height. We have chosen a level below the center of mass of the plume for the second trajectory, as wind direction changes are usually most pronounced closer to the surface. The choice of height for the second trajectory is quite ad hoc, and we have just chosen a height that is 0.5 σ_z below the center of mass of the plume. Furthermore, half of the emission mass from the point source is supposed to follow the center of mass of the plume and half to follow the lower trajectory. Trajectories and travel (aging) time are calculated for plume releases from the point sources at 5 minutes intervals. Hourly concentrations at a certain grid point are calculated using all released parcels that reach that grid point within the specific time period. There is a wealth of σ_y and σ_z formulas available in literature. Algorithms for $\sigma_{y,z}$ can generally be divided into three groups: methods based on power law functions (e.g. Briggs (1974) classical interpolation formulas), methods based on statistical parameters, such as horizontal and vertical direction variances (e.g. Draxler (1976)), and methods based on similarity theory (e.g. Berkowicz et al. (1985)). With standard deviation formulas for the lateral spread (σ_y) as proposed by Briggs (1974), Draxler (1976) or Berkowicz et al. (1985), it appears that the measured lateral spread increases faster downwind in a complex terrain area than is predicted by ordinary σ_y (x)-algorithms, see Andrén (1987). This might be due to wind-direction shear in the vertical, a problem that was first treated by Högström (1964). Smith (1965) presented a method that explicitly deals with this effect by extending Högström's result to spectral representation. The derivation was made for the case of a passive tracer in a field of homogeneous turbulence and constant wind direction shear. For the turbulent energy spectra included in the derivation, the analytical expression obtained from fitting the experimentally measured spectra has been used, see Enger (1983) and Andrén (1987).

4. Simulation domain

An extensive field program, the Measurements Of Haze And Visibility Experiment (MOHAVE), was conducted in winter and summer 1992 in the southwest U.S. The main objectives of the program were to investigate and identify the possible short- and long-term impacts of atmospheric pollutants from major urban areas and industrial sources on the Grand Canyon and its vicinity. A meteorological network of surface and upper-air stations was set up in the region to characterize atmospheric transport.

The outermost model domain was chosen to be the same as for the MM5 simulations, i.e., between 112°W and 116°W, and between 34.51°N and 36.89°N with the center of the model domain at 35.7°N and 114.0°W. The model was run with 123 x 90 grid points in

the horizontal, giving a horizontal resolution of 3 km within the model domain. In the vertical, 30 terrain-following levels have been chosen, ranging from 4 meters above the surface up to 12 000 m ASL.

The area is characterized by a complex topography of river and dry valleys as well as high plateaus. The main land category at altitudes below 6000 feet is desert with bushes. Forest (first juniper, higher up pines) is dominant at altitudes above 6000 feet. There are some artificial lakes in the area, such as Lake Mead.

The surface's elevation, roughness length, vegetation type, albedo, emissivity, and leaf area index are calculated by using landuse data. We have used the North America land cover characteristic database with 1 km resolution. The North America land cover database is one portion of a global land cover characteristic database that is being developed on a continent-by-continent basis. All continents in the global data base share the same map projections (Interrupted Goode Homolosine and Lambert Azimuthal Equal Area), have 1-km nominal spatial resolution, and are based on 1-km AVHRR data spanning April 1992 through March 1993. Each continental database has unique elements that are based on the salient geographic aspects of the specific continent. In addition, a core set of derived thematic maps produced through the aggregation of seasonal land-cover regions are included in each continental database. We have been using the IGBP Land Cover Classification and the Lambert Azimuthal Equal Area projection. The IGBP land cover classification is using 17 different vegetation types, namely:

- Evergreen Needleleaf Forest
- Evergreen Broadleaf Forest
- Deciduous Needleleaf Forest
- Deciduous Broadleaf Forest
- Mixed Forest
- Closed Shrublands
- Open Shrublands
- Woody Savannas
- Savannas
- Grasslands
- Permanent Wetlands
- Croplands
- Urban and Built-Up
- Cropland/Natural Vegetation Mosaic
- Snow and Ice
- Barren or Sparsely Vegetated
- Water Bodies

5. Description of the field program

The field experiment performed in the area during 1992 was sponsored, designed and implemented as a partnership between the Environmental Protection Agency (EPA),

Southern California Edison, and the National Park Service with technical support from a number of government, academic, and industrial organizations. The field study consisted of two intensive monitoring periods (January 4, 1992 to February 13, 1992 and July 7, 1992 to August 31, 1992), which included monitoring of PM2.5 aerosol and SO_2 at over thirty locations, optical monitoring at 10 locations, plus extensive augmentation of the surface and upper air meteorological monitoring throughout the region. The intensive monitoring periods also featured the continuous release from a few locations of perfluorocarbon compounds as tracers to investigate transport and dispersion.

PFTs used in the Project MOHAVE are fully fluorinated hydrocarbons with low solubility in water and moderate vapor pressure, that are therefore inert and non-depositing, as well as non-toxic. The PFT ortho-perfluorodimethylcyclohexane (oPDCH) was released continuously from the stack of MPP during the 30-day winter and 50-day summer intensive periods. Forty-five percent of the oPDCH consist of the isomer ortho-cis (oc)PDCH, which has a background of about 0.52 parts per quadrillion (10^{-15}) or femtoliters per liter (fL/L). The tracer was released from the MPP stack at a rate proportional to the power production. The tracer release rate was constant when the power production stayed within a 10% range of maximum load. For example, if power production was between 90% and 100% of capacity, oPDCH release rate would be at their maximum and constant. If the power production dropped to between 40% and 50% of capacity, tracer release rates would be reduced to one-half the maximum rate. For the summer, accurate SO_2 emissions measurement were not available; however the winter emissions monitoring showed a high correlation ($r^2=0.99$) of emissions with power production. Thus, power production is a good predictor for SO_2 emission rate. For the summer, the ratio of power production to tracer release rate had a standard deviation of 6.9% and r^2 of 0.83. The nearly constant ratio between tracer and SO_2 release allowed the calculation of the estimated amount of co-emitted sulfur associated with a given tracer concentration. This is the concentration of MPP sulfur that would be present in the absence of deposition and other atmospheric loss mechanisms. The full load oPDCH emission rate was about 40 mg/s, which for two extended periods in the winter intensive and one in the summer intensive dropped to about half of that rate. The emissions ratio R of SO_2 to ocPDCH at MPP was maintained throughout the experiment such that the virtual concentration of 650 ng S/m^3 STP should accompany each 1 fL/L of ocPDCH. The average SO_2 to ocPDCH release ratio from MPP was 78.1 g SO_2/mg ocPDCH (488000 moles SO_2/mole ocPDCH) in winter and 73.3 g SO_2/mg ocPDCH (455000 moles SO_2/mole ocPDCH) during summer.

Meteorological monitoring is necessary to characterize the speed, direction, and depth of air mass transport in the region and for model validation and initialization. The existing network of National Weather Service (NWS) and other monitoring sites in the region was insufficient to characterize the complex meteorological setting of the study area. Additionally, for the sparse network of NWS upper air measurement sites, vertical profiles are taken only twice per day. Thus, they do not capture potentially important changes in meteorological conditions, such as the full resolution of a diurnal cycle. While it was recognized that it would be impossible with available funds to set up a meteorological monitoring network to capture all flows of interest, the existing network was supplemented with additional measurement sites.

The additional sites had both surface and upper-air measurements. They consisted of doppler wind profiling radars (915 MHz), Radio Acoustic Sounding Systems (RASS), doppler sodars, and rawinsondes for upper air measurements and typically, wind speed and direction, temperature, relative humidity, and pressure for surface measurements. The radar wind profilers allow for continuous remote sensing of the three components of wind (u, v, and w) from about 100 m to 3-4 km or so above surface, with the maximum height being roughly proportional to absolute humidity. Data is reported as hourly averaged values of horizontal wind speed and direction and vertical velocity for 100 m thick layers at the high resolution mode and 400 m thick layers at the low resolution mode. At the higher levels, the 400 m mode provides greater data recovery than the 100 m mode. The RASS gives virtual temperature profiles by measuring the vertical distribution of the speed of sound using the scatter of radar waves from the vertically propagating acoustic waves (Neff, 1990). The RASS has a range of about 150 m to 600 m with a resolution of about 50 m.

The rawinsonde data of wind speed, wind direction, temperature, relative humidity (RH), and pressure from near the surface to 5000-6000 m AGL are used in this study. The resolution for wind speed and direction measurements was typically 50-100 m, while the resolution of temperature, RH, and pressure measurements was generally 20-30 m. The measurements were usually made twice per day, although sometimes a third was made. Surface meteorological measurements were also made at the optical monitoring sites and SCE's long-term air quality monitoring sites. Data from all National Weather Service monitoring sites in the study region were also archived and added to the Project MOHAVE database. During the summer, the US Army radiosondes at Yuma, normally used only 5 days per week were augmented to 7 days per week. Although not sponsored by Project MOHAVE, additional radar wind profilers were also operated in Southern California during the summer intensive study; data from these profilers was included in the Project MOHAVE database.

In order to have more case studies to test the dynamic higher-order closure model (the MIUU model) a data set from a field experiment performed in the northern part of Sweden has been used. This field experiment is a part of a project granted from NFR in Sweden (Wave-turbulence meso-scale dynamics over complex terrain: Modeling, observation and parameterization. Contract number: G-AA/GU 1247-300). During spring 1999 a field experiment was performed in the north of Sweden. The site is situated between Stora Sjöfallet and Suorva in the southeast, and Akkajaure and Ritsem in northwest. The valley bottom is at about 440 m above sea level, while the surrounding mountains are 1400-2000 m high. The width of the valley is 2-3 km in the narrowest parts and 9 km in the wider parts. A lot of measurements were performed during the campaign: radio soundings 3 times a day, and pilot balloon tracking were performed at three sites every hour during the day-time. The pilot balloon measurements were performed across the valley - in the narrowest part – but also during some occasions along the valley. Furthermore measurements of wind and temperature profiles were made in a 35-m high tower situated in Suorva (the narrowest part of the valley). Winds were also measured in a 35-m tower at 900-m elevation. Furthermore, two automatic weather

stations run by the Swedish Meteorological and Hydrological Institute (SMHI) is situated in the valley, one at Stora Sjöfallet and one at Ritsem. The pilot balloon measurements and the radio soundings show that the terrain in the area generates a lot of gravity waves.
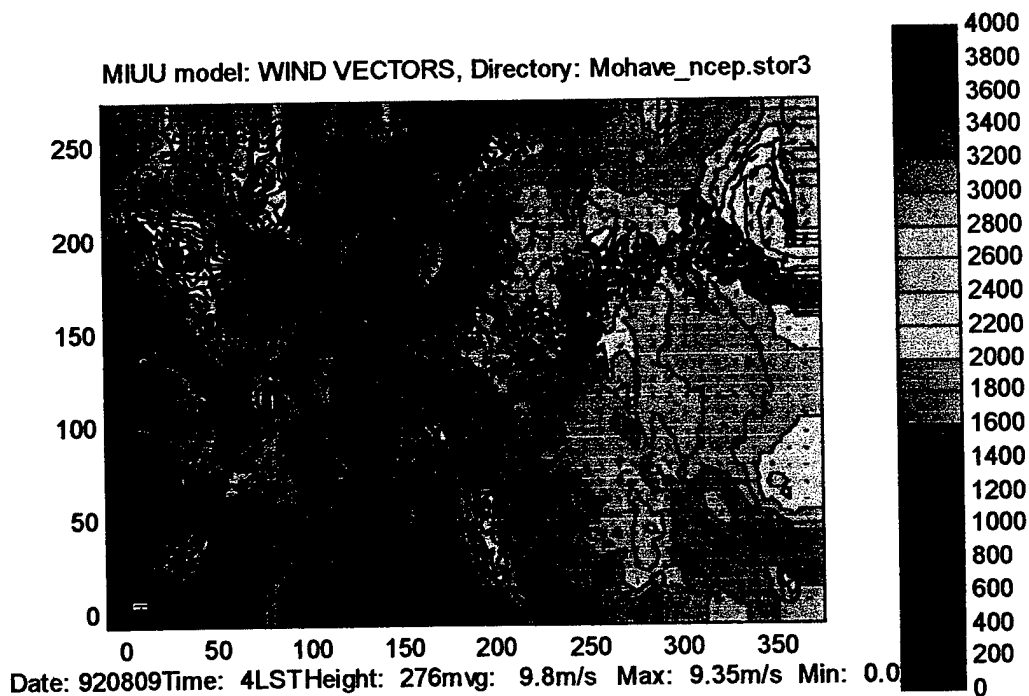
Recent experimental studies have shown that the classical turbulent flux calculation technique is not sufficiently advanced to describe the regimes of strongly stable stratification. To equip the MIUU model with an advanced turbulent flux calculation technique, an advanced similarity theory for the wind and temperature profiles in the stably stratified atmospheric surface layer (ASL) is developed with considerations of the effect of the free-flow static stability on the ASL. In the revised log-linear profiles, empirical coefficients traditionally considered as universal constants, become functions of the Brunt-Väisälä frequency in the free flow and the surface-layer parameters. This new formulation leaves room for occurrence of well-developed turbulence at much larger Richardson numbers, Ri, than had been suspected. Moreover, it results in a pronounced dependence of the turbulent Prandtl number on Ri over a wide range of Ri including the z-less stratification layer, in correspondence with long-standing empirical evidence. The traditional similarity theory disregards the above essential features of the stably stratified ASL. New data from measurements over a slightly inclined plateau provide experimental support for the proposed theory (Zilitinkevich, S., and Calanca, P., 2000).

6. Realized simulations with the MIUU model:

The MIUU model was run for the same time period as the other models, i.e., from 12 UTC on August 5, 1992, to 12 UTC on August 14, 1992. The model was run continuously for 216 hours.

The output of the meteorological model will be verified against the meteorological measurements described above. The meteorological fields from the model will then be used as input to the dispersion model described above.

The figure below shows the MIUU model results at 276 m AGL for 4:00 local time on August 9, 1992. The figure clearly shows a nocturnal jet in the center of the Colorado - river valley with northerly flow parallel to the valley.

10

MIUU model: WIND VECTORS, Directory: Mohave_ncep.stor3

Date: 920809Time: 4LSTHeight: 276mvg: 9.8m/s Max: 9.35m/s Min: 0.0

7. Trajectory modeling

Graduate student Dong-Chul Kim was working on a trajectory model during this year. Using the three-dimensional wind field predicted by MM5, this model can trace the center of the tracer blob both forward and backward. Tracer plume (the streak line) at a certain time t can be obtained by running the trajectory model multiple times with tracers released at successive times, from t-nΔt to t-Δt. The following two figures show the trajectory of a blob released at 400m level from MPP on August 10, 1992. The first one shows the trajectory on latitude-longitude coordinates with terrain contours and the other shows the longitude-altitude cross section of the trajectory. A FORTRAN program for evaluating the tracer potential of the trajectory model output is also completed. A sensitivity test is under way to check the sensitivity of the trajectories to the wind speed, wind direction and the height of the initial plume rise.

11

Pressure of Trajectory

w = 0.1 m/s
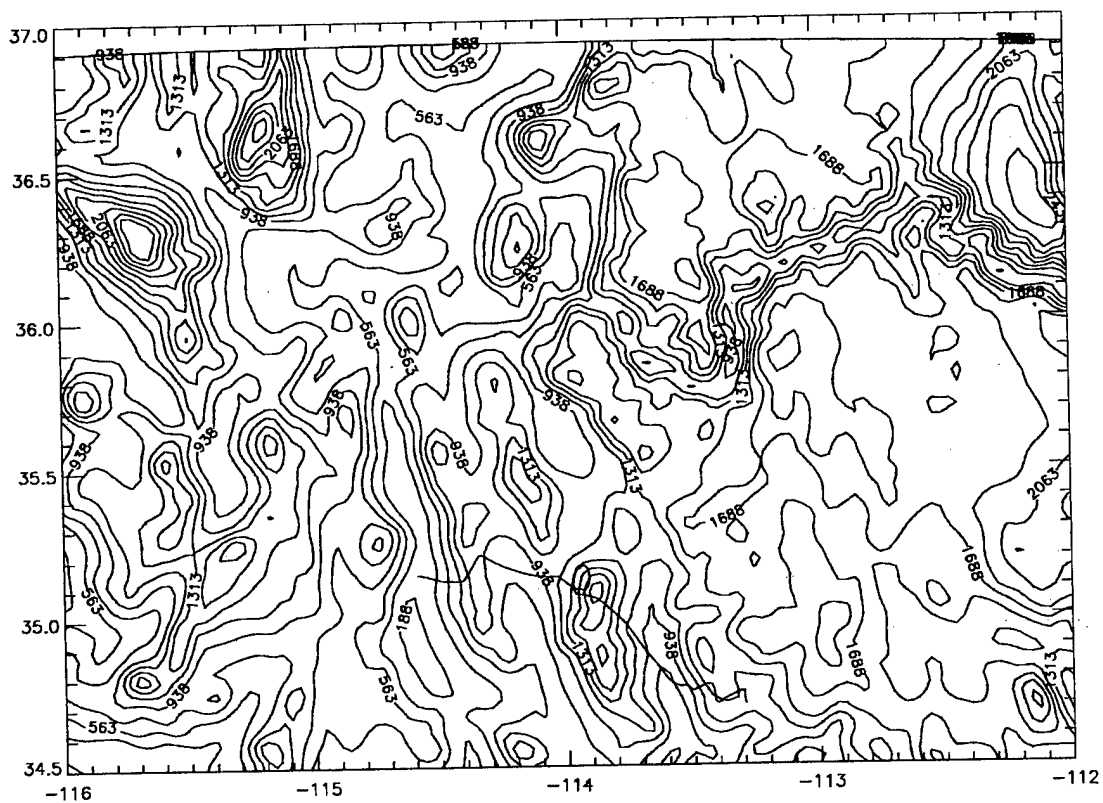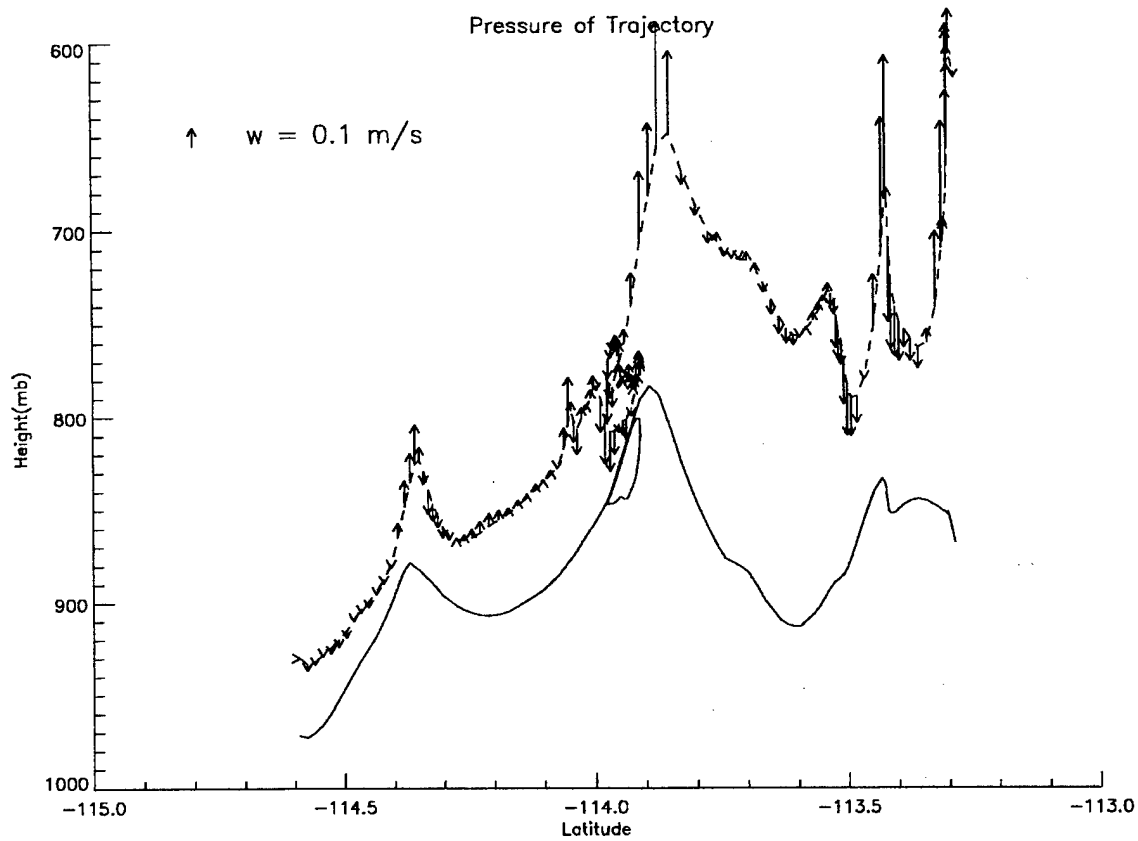
8. Future work

The majority portion of the present project is a part of two Ph.D. theses. One dealing with the dynamics in mountain areas (Matthias Mohr, Uppsala University, Sweden), and the second one dealing with dispersion in complex terrain (Babatunde Abiodun, Federal University of Technology in Akure, Nigeria and Uppsala University, Sweden).

Future work will include (among others):

- Detailed verification of the MIUU model results against measurements
- Testing of new parameterizations, mainly for the stably stratified boundary layer
- Comparison of different dispersion-meteorology modeling combinations

7a. Comparison method

Usually one examines model simulations with measured data by statistically examining the agreement between measured and simulated data. This will also be performed for the different dispersion-meteorology modeling combinations in this study. The comparisons will be performed for different long mean-value periods, from 1 day mean values up to entire intensive periods. The different model combinations are:

- HOCD-model + MIUU-model
- SGTD-model + MIUU-model (3 different horizontal resolutions -- 6 km, 3 km, and 1.5 km)
- SGTD-model + MM5-model (only for a 8 days period during summer intensives)
- SGTD-model + CALMET-model
- SGDT-model + WP-model (from 4 wind profilers, see section 2.3)
- SGDT-model + wind profiler only at MPP

Perhaps a better method of examining a model's consistency with "reality" is to designate a measure of a modeling system's disagreement with the measured data. An initial verification is to examine if the plume is passing the measuring site (Index I_p) -- either at surface or at a higher elevation. Another possible method is to calculate the distance in space where measurements and simulations agree with each other.

Index $I_P =$	1	if plume above the measurement site and measured concentration > 0
Index $I_P =$	$(\pi/2 * R - \Delta s)/(\pi/2 * R)$	if plume not above measurement site and measured concentration > 0

where R is the radius of a circle around the source, which is the distance between the source and a measuring site; Δs is the distance on that circle between measuring site and the plume edge (concentration higher than a threshold value). This means that index I_P has values between -1 and $+1$, with value $+1$ if the plume passes the site and with value -1 if simulated plume goes in an opposite direction of the site.

Calculating the smallest distance between the measured concentration to a point, below the simulated plume centerline height, which has the same concentration gives three distances:

- Δs distance in angular direction
- Δr distance in radial direction
- Δz distance in vertical direction

from which we can define three indexes, I_S, I_R, and I_Z.
Index $I_S = \Delta s / (\pi * R)$; index I_S has values between 0 and 1, with 0 best having the agreement

Index $I_R = \Delta r / R$; index I_R between 0 and 1, with 0 having the best agreement

Index $I_Z = \Delta z / Z_c$; Z_c =plume centerline height, index I_Z between 0 and 1, with 0 being the best.

Furthermore, we will compare the different model combinations with each other by looking at the agreement or disagreement between the models statistically.
The following statistical parameters were calculated within a horizontal domain of 300 km x 250 km:

- Mean concentration at the surface for the whole domain
- Mean concentration integrated up to the top of the model for the whole domain
- Number of grid areas (1x1 km^2) with concentrations above a certain threshold at the surface.
- Number of grid areas with concentrations above a certain threshold covered by both models at the surface.
- Intersection area (area that is covered by both models in either model).

References

Andrén, A., 1987: A combined first-order closure/Gaussian dispersion model. *Atmos. Environ.*, **21**, 1045-1058.

Berkowicz, R., H.R. Olesen, and U. Torp, 1985: The Danish Gaussian air pollution model (OML): description, test and sensitivity analysis in view of regulatory applications. 15th International Technical Meeting on Air Pollution Modeling and its Application, St Louse, U.S.A., 16-19 April, 1985.

Briggs, G.A., 1974: Diffusion estimation for small emissions. In USAEC report ATDL-106, National Oceanic and Atmospheric Administration.

Davies, H.C., 1976: A lateral boundary formulation for multi-level prediction models. *Quart. J. Roy. Meteor. Soc.* **102**, 405-418.

Davies, H.C., 1983: Limitations on some common lateral boundary schemes used in regional NWP models. *Mon. Weather Rev.* **11**, 1002-1012.

Draxler, R.R., 1976: Determination of atmospheric diffusion parameters. *Atmos. Environ.*, **10**, 99-105.

Draxler, R.R., R.N. Dietz, F.J. Lagomarsino, and G. Start, 1991: Across North America Tracer Experiment (ANATEX): Sampling and Analysis, *Atmos. Environ.*, **25A**, 2815-2836.

Enger, L., 1983: Numerical boundary layer modeling with application to diffusion -- II. A higher order closure dispersion model. Department of Meteorology, University of Uppsala, Sweden, report No. 71

Enger, L. and D. Koracin, 1995: Simulations of dispersion in complex terrain using a higher-order closure model. *Atmos. Environ.*, **29**, 2449-2465.

Grell, G.A., J. Dudhia, and D.R. Stauffer, 1995: A description of the fifth-generation Penn State/NCAR Mesoscale Model (MM5), NCAR Tech. Note TN-398, 122 pp.

Högström, U., 1964: An experimental study on atmospheric diffusion. *Tellus*, **16**, 205-251.

Jensen, T.G., 1998: Open boundary conditions in stratified ocean models. *J. of Marine Systems* **16**, 297-322.

Kalnay, M., Kanamitsu, and W.E. Baker, 1990: Global numerical weather prediction at the National Meteorological Center. *Bull. Amer. Meteor. Soc.*, **71**, 1410-1428.

Kanamitsu, M., 1989: Description of the NMC global data assimilation and forecast system. *Wea. and Forecasting*, **4**, 335-342.

Kanamitsu, M., J.C. Alpert, K.A. Campana, P.M. Caplan, D.G. Deaven, M. Iredell, B. Katz, H.-L. Pan, J. Sela, and G.H. White, 1991: Recent changes implemented into the global forecast system at NMC. *Wea. and Forecasting*, **6**, 425-435.

Neff, W.D., 1990: Remote sensing of atmospheric processes over complex terrain. In Atmospheric Processes over Complex Terrain. W. Blumen, editor. American Meteorological Society, Boston, MA. USA, 173-228.

NMC Development Division, 1988: Documentation of the research version of the NMC Medium-Range Forecasting Model. NMC Development Division, Camp Springs, MD, 504 pp.

Scire, J.S., E.M. Insley, R.J. Yamartino, and M.E. Fernau, 1995: User's guide for the CALMET Meteorological Model. USDA Forest Service Tech. Rep. 1406-01, Cadillac, MI, by Earth Tech, Concord, MA.

Smith, F. B., 1965: The role of wind shear in the horizontal diffusion of ambient particles. *Q. Jl. R. met. Soc.*, **91**, 318-329.

Vimont, J., 1997: Evaluation of the CALMET/CALPUFF modeling system using Project MOHAVE tracer and implications for sulfate contributions. Proc. Visual Air Quality Conference, Sept 9-12, 1997, Barlett, NH, 436-446.

Zilitinkevich, S. and Calanca, P., 2000: An extended similarity-theory for the stably stratified atmospheric surface layer. Accepted for publication in *Quart. J. Roy. Meteorol. Soc.*

REPORT DOCUMENTATION PAGE

Public reporting burden for this collection of information is estimated to average 1 hour per response, including the time for reviewing instructions, searching existing data sources, gathering and maintaining the data needed, and completing and reviewing the collection of information. Send comments regarding this burden estimate or any other aspect of this collection of information, including suggestions for reducing this burden, to Washington Headquarters Services, Directorate for Information Operations and Reports, 1215 Jefferson Davis Highway, Suite 1204, Arlington, VA 22202-4302, and to the Office of Management and Budget, Paperwork Reduction Project (0704-0188), Washington, DC 20503.

1. AGENCY USE ONLY (Leave Blank)	2. REPORT DATE	3. REPORT TYPE AND DATES COVERED
	Augus 28, 2000	Annual: 05/01/99 - 04/30/00

4. TITLE AND SUBTITLE
Modeling the dispersion of vapor and aerosol particulates in the atmospheric boundary layer

5. FUNDING NUMBERS
G N00014-98-1-0557

6. AUTHORS
Steven K. Chai

7. PERFORMING ORGANIZATION NAME(S) AND ADDRESS(ES)
Desert Research Institute
University & Community College System of Nevada
2215 Raggio Parkway
Reno, NV 89512-1095

8. PERFORMING ORGANIZATION REPORT NUMBER
N/A

9. SPONSORING / MONITORING AGENCY NAME(S) AND ADDRESS(ES)
Office of Naval Research
800 North Quincy Street
Arlington, VA 22217-5660

10. SPONSORING / MONITORING AGENCY REPORT NUMBER

11. SUPPLEMENTARY NOTES
None

12a. DISTRIBUTION / AVAILABILITY STATEMENT
Unlimited

12b. DISTRIBUTION CODE

13. ABSTRACT (Maximum 200 words)
Report attached.

14. SUBJECT TERMS
Disprsion Modeling
Bouindary Layer
Complex Terrain

15. NUMBER OF PAGES
17

16. PRICE CODE

17. SECURITY CLASSIFICATION OF REPORT	18. SECURITY CLASSIFICATION OF THIS PAGE	19. SECURITY CLASSIFICATION OF ABSTRACT	20. LIMITATION OF ABSTRACT
Unclassified	Unclassified	N/A	

NSN 7540-01-280-5500

DTIC QUALITY INSPECTED 4